Desalination and Water Treatment
www.deswater.com
doi: 10.5004/dwt.2021.27386

229 (2021) 17–30
July

Modeling, simulation, and optimization of the membrane performance of seawater reverse osmosis desalination plant using neural network and fuzzy based soft computing techniques

Rajesh Mahadeva[a], Mahendra Kumar[b], Gaurav Manik[a,*], Shashikant P. Patole[c]

[a]*Department of Polymer and Process Engineering, Indian Institute of Technology, 247667 Roorkee, Uttarakhand, India, Tel. +91-1322714340; email: gaurav.manik@pe.iitr.ac.in (G. Manik), Tel. +91-9909030497; email: rmahadeva@pe.iitr.ac.in (R. Mahadeva)*
[b]*Department of Electrical Engineering, Indian Institute of Technology, 247667 Roorkee, Uttarakhand, India, Tel. +91-7014798426; email: mkumar1@ee.iitr.ac.in (M. Kumar)*
[c]*Department of Physics, Khalifa University of Science and Technology, Abu Dhabi 127788, United Arab Emirates, Tel. +971-501335164; email: shashikant.patole@ku.ac.ae (S.P. Patole)*

Received 15 December 2020; Accepted 30 April 2021

ABSTRACT

One of the challenging tasks in desalination plants is to manage and optimize their real-time performance. In this direction, soft computing techniques have demonstrated superior efficiency compared to conventional techniques in overcoming this problem and predict optimal process conditions. In this paper, artificial neural network (ANN), particle swarm optimization assisted ANN (PSO-ANN), fuzzy inference system (FIS), and adaptive neuro-fuzzy inference system (ANFIS) models have been developed to predict the membrane performance of the seawater reverse osmosis (SWRO) desalination plants. All developed models consisted of four input parameters: feed temperature (5°C–30°C), feed pressure (45–65 kgf/cm^2), feed flow rate (~30 L/min), and feed total dissolved solids (TDS) (~32,000 ppm) with two output parameters: permeate flow rate (2.8–8.8 L/min) and permeate TDS (45–121.6 ppm). The models so obtained and trained produced a fairly good agreement between the experimental and predicted dataset. Amongst all models simulated, the PSO-ANN model provides superior performance for permeate flow rate and TDS (R^2 = 0.998, 0.997) with minimum errors (MSE = 0.007, 1.783) compared to other models (ANN, FIS, and ANFIS). Future results suggested that models may serve as perfect diagnostic tools for designing SWRO desalination plants to reduce the Capex, Opex, time, and energy.

Keywords: Artificial neural network; Fuzzy inference system; Particle swarm optimization assisted ANN; Seawater reverse osmosis; Adaptive neuro-fuzzy inference system

1. Introduction

1.1. Importance of water and desalination

Water and desalination share a close relationship with each other, and the latter playing an important role in human life by offering a continuous supply of pure drinking water. In the present scenario, due to population growth worldwide, conventional freshwater sources (i.e., rivers, streams, ponds, lakes, reservoirs, and ground waters) have either been completely destroyed or are limited in their supply of drinking water at a specific location. This has increased water scarcity, which inversely affects the agriculture, industry, animal, and human development [1–5]. However, optimal exploitation of seawater is one of the most emerging alternative resources to solve water crises. With ~97% source of water of earth, seawater can be utilized to generate freshwater through various desalination

* Corresponding author.

techniques such as multi-effect distillation (MED), reverse osmosis (RO), and multi-stage flash (MSF). Among them, RO is the most versatile, influential, and widely used (>63%) technique worldwide [1,6–8]. It has demonstrated a remarkable potential for a cost-effective operation, maintenance free, and controlled desalination process over the last 60 y [9]. This has prompted several researchers and scientists across the globe to focus and contribute to this emerging field.

1.2. Literature survey using soft computing techniques

Currently, the demand for designing and running seawater desalination plants has increased worldwide and this has prompted immense interest in the soft computing modeling approach to represent and simulate accurate plant performance [10]. Until now, such advanced techniques have helped the development of several deterministic and stochastic models, such as a porous model, irreversible thermodynamic model, the membrane resistance model, and solution diffusion model [11,12]. Some of such techniques face some challenges such as high computational time, standard rules, and formulation of meaningful input/output datasets for process analysis. However, much advanced soft computing models developed recently involve intelligent computation to reduce simulation time and ability to deal with difficult situations [13].

Chau [14] has developed a particle swarm optimization-assisted ANN (PSO-ANN) model for an accurate water stage forecast of Shing Mun River, Hong Kong. The model predicted improved results (R^2 = 0.99) than the BP-ANN model (R^2 = 0.96) for 1 d datasets. Buyukyildiz et al. [15] have presented five approaches, including PSO-ANN, multi-layer ANN, support vector regression, radial basis neural network, and adaptive neuro-fuzzy inference system (ANFIS), to estimate water level (monthly) change in Lake Beysehir, Turkey. Alizamir and Sobhanardakani [16] developed an PSO-ANN and ANN-bayesian regulation (BR) models to predict heavy metals (Zn, Pb, As, and Cu) contamination in groundwater of Toyserkan Plain, Hamedan Province, Iran. They observed that the PSO-ANN model was more precise and accurate than the ANN-BR model to predict heavy metals in the groundwater. Sulugodu and Deka [17] evaluated streamflow forecasting performance using soft-computing methods such as ANFIS and PSO-ANN. Three decades of rainfall datasets (CHIRPS satellite provided rainfall data) from 1983 to 2012 over the Nethravathi Basin, Karnataka, India, were used for analysis. The investigation was carried out from June to September (monsoon season), out of which 70% datasets were considered for training and the remaining 30% for testing. Such machine learning influenced models have been reported earlier to intelligently enable learning from experiments for understanding system behavior accurately and help in the smoother running of processes [9,10,18–22]. Literature suggests that the modeling parameters (i.e., number of swarm size, number of the hidden layer, hidden layer nodes, the weight of inertia, acceleration factors, etc.) play a major role in designing soft computing models. Also, selecting these parameters varies according to the dataset size, pattern, and proper format. Thus, this work attempts to iteratively find the best parameters by the hit and trial error methods. Moreover, based on past efforts, the literature [16,17] has also suggested initial robust and useful parameters for such modeling studies.

1.3. Objectives and contributions

The purpose of this research is to develop computationally fast and accurate models using neural network and fuzzy-based soft computing techniques (ANN, PSO-ANN, FIS, and ANFIS) for analyzing the membrane performance of the seawater desalination plant in several working conditions. The ANN and PSO-ANN models are based on programming and learning algorithms. ANN has been adapted to learn by backpropagation (BP), while PSO-ANN supports learning by PSO. Besides, FIS and ANFIS are rule-based models that have been formed upon the conversion of available inputs into crisp fuzzy inputs. The resulting models can quickly and intelligently learn the key information from the experimental datasets and possess the capabilities to predict outputs accurately. Furthermore, the study explores optimum system parameters using the developed models and suggests a smart/optimized desalination plant with reduced Capex, Opex, process time, and energy.

In general, Fig. 1. illustrates a typical breakdown of the clean water production costs of the seawater reverse osmosis (SWRO) plant [23]. It has been compiled based on a comparative review of over 50 desalination plants around the world (mainly in the USA, Australia, Europe, the Middle East, and the Caribbean) [23]. Although, the cost component varies according to the size and the location of the plant. The largest expenditure (30%–40%) usually the direct Capex (i.e., construction cost), while the indirect Capex (10%–20%) includes for project engineering, finance, and development. Besides, 20%–35% cost involves in the energy requirements. The operational and other maintenance costs (Opex) apply around 15%–30% for the water production [6,23].

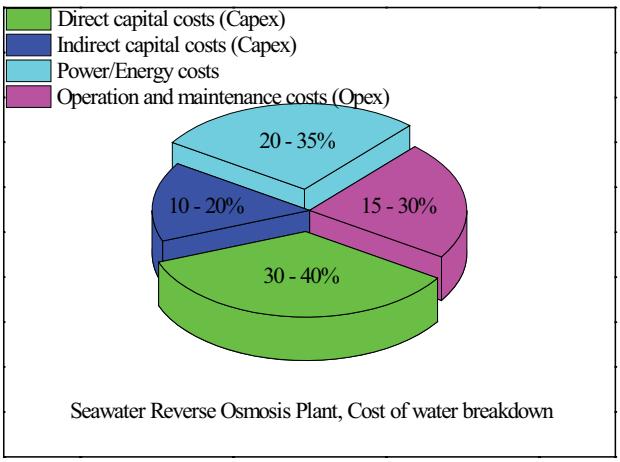

Fig. 1. Typical cost of water breakdown for the SWRO desalination plant [6,23].

2. Data description

Lee et al. [10] have studied the SWRO desalination pilot plant to investigate and interpret membrane performance with varying seawater parameters. They used the commercial spiral-wound RO membranes (6.9 m^2 transfer area) for the experiments. The operating range of input feed parameters consisting of temperature, pressure, flow rate and TDS, and outputs of permeate flow rate and TDS have been expressed in Table 1. The salt concentration and permeate flow rate were measured using the conductivity and flow meters, respectively.

3. Model development

3.1. ANN modeling

An ANN is a self-learning computing system designed to simulate the accurate prediction of permeate flow rate and TDS of the seawater desalination plant. It is the substance of artificial intelligence (AI), which solves the problems that would be difficult/impossible by human or statical standards. Fig. 2. presents the graphical diagram of a three-layer feedforward neural network model. Here, all previous layer nodes have been linked to all nodes of the next layers implemented using MATLAB's Neural Network Toolbox. The input layer with four nodes consists of feed temperature, feed pressure, feed flow rate, and feed TDS of the system, while an output layer consists of two nodes (permeate flow rate and TDS) and one hidden layer with variable (n) nodes. The entire dataset of the system has been divided into three parts: training (70%), validation (15%), and remaining for testing (15%), and the training datasets have been referred to as a set of patterns [9].

Table 1
Description of parameters involved in the SWRO desalination plant [10]

	Parameter	Number	Range
Feed	Temperature, T_f, °C	30	5–30
	Pressure, P_f, kgf/cm²	30	45–65
	Flow rate, F_f, L/min	30	29.6–30.2
	TDS, C_f, ppm	30	31,300–32,100
Permeate	Flow rate, F_p, L/min	30	2.8–8.8
	TDS, C_p, ppm	30	45.0–121.6

The developed neural network model's output of the hidden layer nodes, H_j^p and the system's final outputs, $\hat{y}_k^p$ can be calculated by Eqs. (1) and (2), respectively [24]:

$$H_j^p = f\left(w_{0j} + \sum_{i=1} w_{ij}^h x_i^p\right) \tag{1}$$

$$\hat{y}_k^p = f\left(w_{0k} + \sum_{j=1} w_{jk}^0 H_j^p\right) \tag{2}$$

where x_i^p are the network inputs, w_{ij}^h are the weights between the input and hidden layers, w_{jk}^0 are the weights between the hidden and output layers, w_{0j} and w_{0k} are the bias, p prefers to the pattern, and i, j, and k are the number of the input, hidden, and output nodes, respectively.

The hidden layer nodes' output has been calculated using a sigmoid transfer function, $f(x)$ used as an approximation function. It is calculated from its personal derivative at any point and produces outputs between 0 and 1 as the input goes from negative to positive infinity, as shown in Eq. (3).

$$f(x) = \frac{1}{1+e^{-x}} \tag{3}$$

Then the outputs of the hidden nodes are afterward inserted into Eq. (2), and the sigmoid function again computes the output. Lastly, the neural network's final

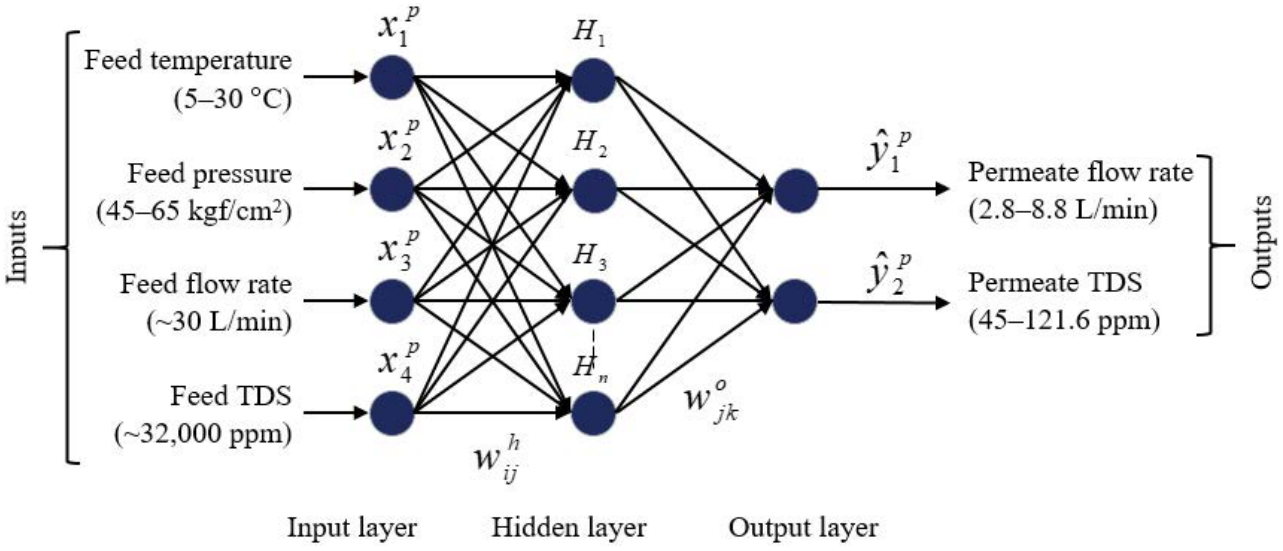

Fig. 2. Graphical illustration of an artificial neural network model.

output, $\hat{y}_k^p$ has been used to calculate the mean square error (MSE) with the real output, y_k^p based on Eq. (4) [24]:

$$\mathrm{MSE} = \min \frac{1}{2N} \sum_{p=1}^{N} \sum_{k=1}^{M} \left(\hat{y}_k^p - y_k^p \right)^2 \tag{4}$$

where N is the number of patterns, and M is the number of output nodes.

As a learning algorithm, we have employed the Levenberg–Marquardt backpropagation (LM-BP) algorithm [24] first to calculate the network's MSE gradient and then find the weights that minimize MSE. In the LM-BP algorithm's training process, the network weights are adjusted to systematically reduce the errors, causing a good promise between the input values and desired output estimates.

3.2. PSO-ANN modeling

In this PSO-assisted modeling, the ANN model has been optimized by the PSO algorithm for predicting the permeate flow rate and permeate TDS of the seawater desalination plant. Kennedy and Eberhart in 1995 have proposed a computational method (stochastic population-based (swarm/bird/fish/particle) search technique) that optimizes the problems iteratively called PSO [25]. It has been inspired by the social/collective behavior of bird flocking or fish schooling. PSO has initialized by a group of random particles and searches optima nearby in a multidimensional space by updating generations. In every iteration, each particle has updated two best values. The first one is the individual best fitness value obtained by the individual particle called personal best (p_{best}) position and another best value obtained by the neighbor particle called global best (g_{best}) [26,27]. Afterward, finding the two best values (p_{best} and g_{best}), every particle updates its velocity and positions with Eqs. (5) and (6) [28,29]:

$$v_i^{n+1} = \omega v_i^n + c_1 r_1^n \left[x_{i,p}^n - x_i^n \right] + c_2 r_2^n \left[x_g^n - x_i^n \right] \tag{5}$$

$$x_i^{n+1} = x_i^n + v_i^{n+1} \tag{6}$$

where v_i^n, v_i^{n+1} are the velocity of ith particle at nth and n + 1th iteration, respectively; x_i^n, x_i^{n+1} are the position of ith particle at nth and n + 1th iteration; c_1, c_2 are the acceleration factors; r_1^n, r_2^n are the random numbers; ω is the weight of inertia assumed in range of 0–1; x_g^n is the global best (g_{best}); $x_{i,p}^n$ is the individual best (p_{best}); n is the total number of iterations.

Our next step for optimizing modeling is setting up the PSO algorithm's optimum parameters (swarm size, ω, c_1, c_2, and n) before the ANN model. Finally, determine the excellent performance in terms of R^2 and MSE. The same number of input, hidden, and output layer nodes applied as the ANN modeling.

3.3. FIS modeling

FIS modeling is vital to efficiently manage the SWRO desalination system by optimizing the permeate flow rate and TDS. Herein, the designing of the FIS modeling has been accomplished in two steps. In the first step, we have assumed two inputs (feed temperature 5°C–30°C), and pressure 45–65 kgf/cm^2, and a single output (permeate flow rate 2.8–8.8 L/min) (case-1). In another case (case–2), permeate TDS (45–121.6 ppm) has been taken as an output. Feed flow rate ~30 L/min and feed TDS ~32,000 ppm have been considered constant. The designing architecture is based on a Mamdani fuzzy inference system (FIS), which uses the "Centroid" process for defuzzification, giving a crisp output of the system [30]. Here, we have used triangular membership functions (trimf) of the inputs and outputs are illustrated in Fig. 3a–d. It is the most straightforward shape function, defined three parameters for three points: two for the feet and one for the curve's tip.

The FIS model has been planned as follows: The first fuzzy input, feed temperature, has been divided according to the operative temperature range of the plant into five fuzzy subsets presented by five membership functions (MFs) as follows: very small temperature (VST), small temperature (ST), medium temperature (MT), large temperature (LT), and very large temperature (VLT) with the range of values varying from 5°C to 30°C. The second fuzzy input, feed pressure, has been divided into five fuzzy subsets indicated as follows: very small pressure (VSP), small pressure (SP), medium pressure (MP), large pressure (LP), and very large pressure (VLP) with the range of values varying from 45 to 65 kgf/cm^2. The first fuzzy output permeates flow rate has been divided into five fuzzy subsets indicated as follows: very small permeate flow rate (VSF), small permeate flow rate (SF), medium permeate flow rate (MF), large permeate flow rate (LF), and very large permeate flow rate (VLF) lying in 2.8–8.8 L/min range. The second fuzzy output, permeate TDS, has been divided into five fuzzy subsets indicated as follows: very small TDS (VSD), small TDS (SD), medium TDS (MD), large TDS (LD), and very large TDS (VLD) with values lying within the 45–121.6 ppm range.

In FIS assisted modeling, it uses the "IF-THEN" logical operating rules with "AND" or "OR" connectors for the essential decision rules. Thus, step 2 involves defining some fuzzy rules for the predefined input/output parameters and creating appropriate decision matrices. For example, based on an earlier understanding of the considered system, a set of 25 rules have been created for each output and concise by a decision matrix illustrated in Fig. 3e and f. It has been noted that the designing of the FIS modeling consists of the fuzzy IF-THEN rules, choice of MFs, decision matrix, fuzzification, and the defuzzification interface units [30–32]. The defuzzification method helps obtain the best single value from the fuzzy set.

3.4. ANFIS modeling

ANFIS modeling, first proposed by Jang and Sun [33,34], exemplifies a robust soft computing technique that may find great use for the prediction of permeate flow rate and TDS of the seawater desalination plant. The architecture of an ANFIS model involves a five-layered feedforward neural network, illustrated in Fig. 4. The first input layer consists of four input nodes (feed temperature

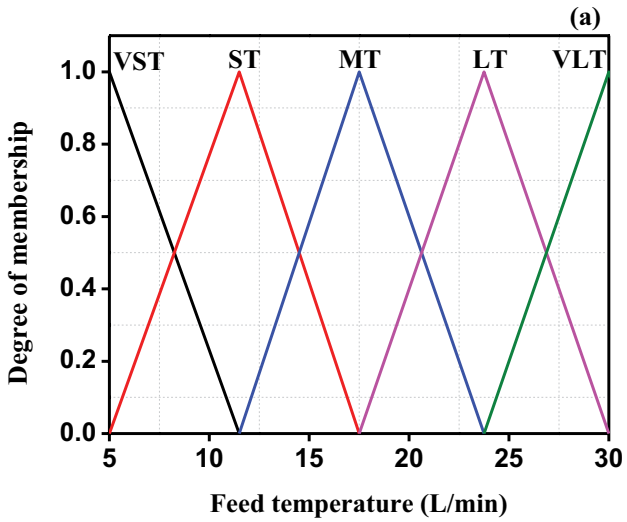

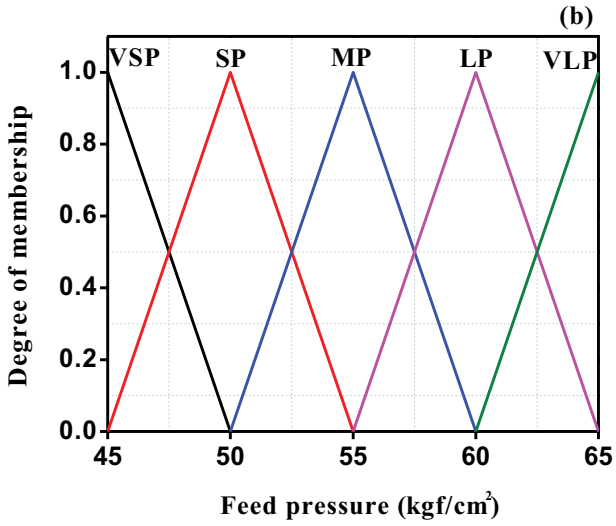

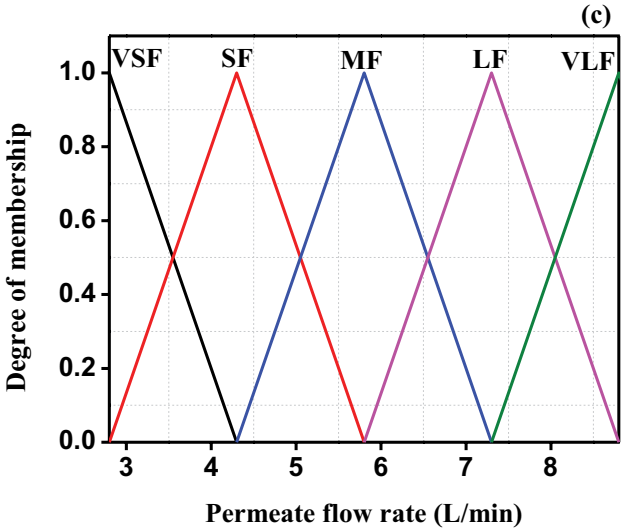

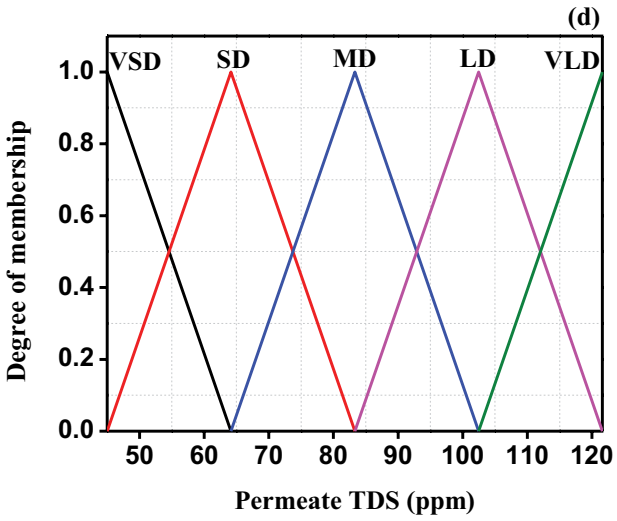

(e)

Temperature \ Pressure	VSP	SP	MP	LP	VLP
VST	VS	S	M	L	L
ST	VS	VS	S	S	M
MT	VS	S	M	L	L
LT	S	M	M	M	L
VLT	S	M	L	L	VL

Fuzzy decision matrix of permeate flow rate (L/min)

(f)

Temperature \ Pressure	VSP	SP	MP	LP	VLP
VST	L	M	S	S	VS
ST	M	S	S	S	VS
MT	L	M	S	S	VS
LT	L	M	M	S	S
VLT	VL	L	M	M	S

Fuzzy decision matrix of permeate TDS (ppm)

Fig. 3. Degree of membership functions of: (a) feed temperature 5°C–30°C, (b) feed pressure 45–65 kgf/cm², (c) permeate flow rate 2.8–8.8 L/min, (d) permeate TDS 45–121.6 ppm, (e) fuzzy decision matrix of permeate flow rate, and (f) fuzzy decision matrix of permeate TDS.

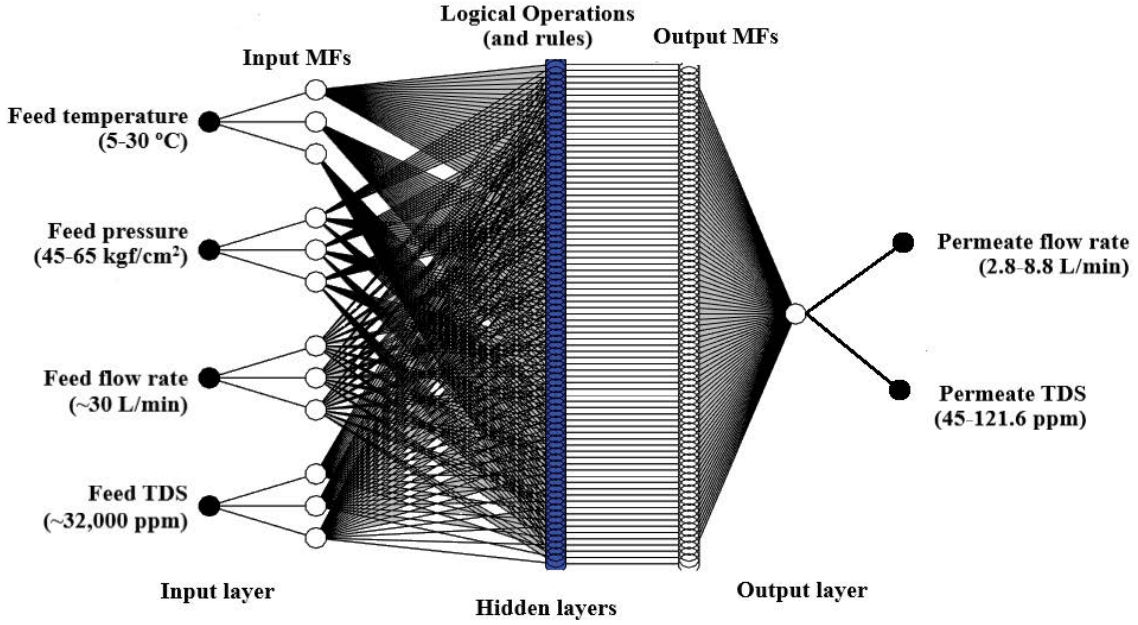

Fig. 4. Structure of the ANFIS with four input nodes constructed 81 fuzzy rules, each for two output nodes: permeate flow rate and TDS.

5°C–30°C, feed pressure 45–65 kgf/cm², feed flow rate ~30 L/min, and feed TDS ~32,000 ppm) and the last output layer consists of two output nodes (permeate flow rate 2.8–8.8 L/min and permeate TDS 45–121.6 ppm) of the structure. Here, we have used 70% of the total data for training, 15% for validation, and the remaining 15% for testing of the system. Hidden layers involve triangular membership functions (trimf), used to determine the system's initial premise parameters. Although the number of MFs assigned to each input variable by trial and error methods. It generates 81 logical operations rules, each for two outputs as per given MFs in the present case. Additionally, Mamdani FIS has been used to achieve the tuning process of the structures. Lastly, the last layer summarized the operation rules and calculated outputs of the plant.

4. Results and discussion

All models (ANN, PSO-ANN, FIS, and ANFIS) have been developed and simulated using MATLAB R2019a software to design the SWRO desalination plant and optimize its performance. The system used had the following configuration: Intel (R) Core (TM) i5-8250U CPU@1.60 GHz, 4 Core(s), 1,801 MHz, 8 Logical processors, and 8.00 GB RAM.

4.1. Models simulation and optimization

4.1.1. ANN model optimization

For the ANN model optimization and analysis, we have performed various simulations. It was found that the ANN model's performance depends upon the number of hidden layer nodes (n). Fig. 5a and b illustrate the experimental datasets for testing the ANN model for permeate flow rate and TDS of the seawater RO desalination plant with variable hidden layer nodes. It has been observed that the number of nodes between 4 and 6 generated relatively very low errors (MSE) and high regression (R^2) for the case of analysis of permeate flow rate. However, the estimates did not show any trend for TDS analysis but were favorable for n = 7. Thus, the simulation indicates that 5 and 7 number of hidden layer nodes are most suitable for predicting permeate flow rate and TDS from the ANN models.

4.1.2. PSO-ANN model optimization

PSO-ANN models, in general, depend upon the choice of swarm size, acceleration factors (c_1 and c_2), the weight of inertia (ω), and also the number of nodes (n) in the hidden layer. Fig. 6a and b illustrate the performance results of the permeate flow rate and TDS of the seawater RO desalination plant with variable swarm sizes 10–70. It is apparent that an optimal swarm size of 40 predicts the best results for both outputs, permeate flow rate, and TDS than others captured in terms of R^2 and MSE. Thus, the minimal swarm sizes will not recognize the problem correctly, while a larger swarm-sized model will tend to confuse and predict maximum errors.

Another critical parameter is ω, which performs an essential role in the optimization of PSO-ANN modeling. In the literature, a large variation in the values of ω has been observed for various applications [15,35,36]. Fig. 7a and b show the permeate flow rate and TDS performance results with a variable ω using PSO-ANN models. A choice of ω = 0.25 displayed the best performance (R^2 = 0.998, MSE = 0.007) for the output permeate flow rate, and (ω = 0.1 + rand × 0.4) exhibited the best performance (R^2 = 0.997, MSE = 1.783) for the output permeate

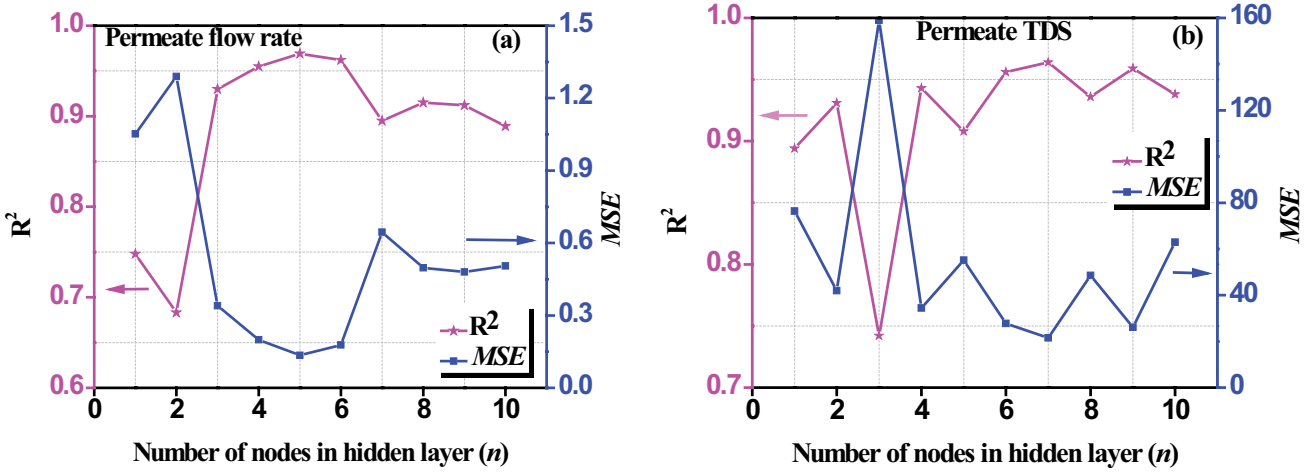

Fig. 5. Illustration of the dependence of simulation errors (MSE) and regression quality (R^2) on the number of nodes in the hidden layer for the case of estimation of: (a) permeate flow rate and (b) TDS using ANN.

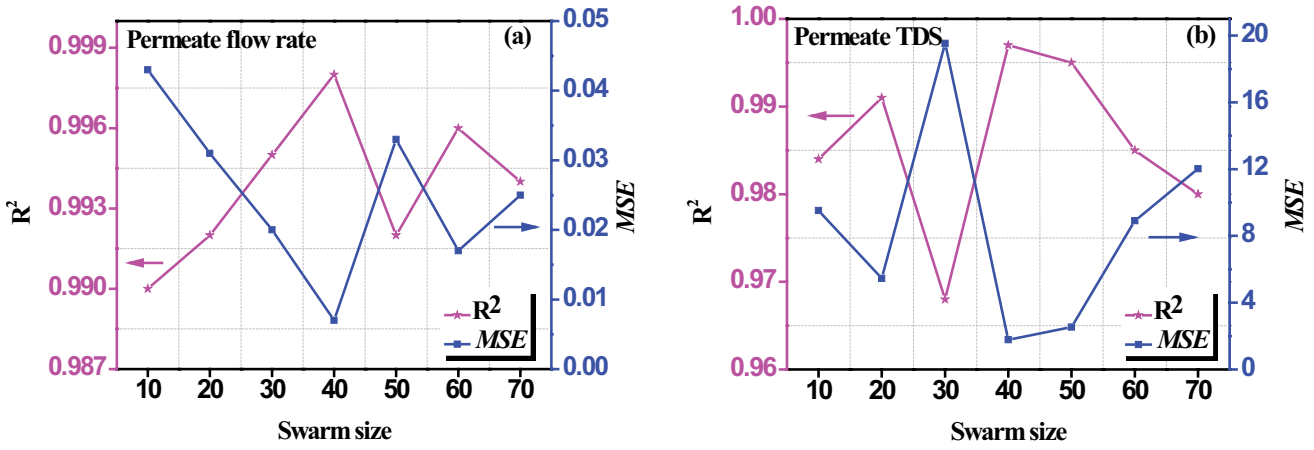

Fig. 6. Illustration of the dependence of simulation errors (MSE) and regression quality (R^2) on the swarm population (size) for the case of estimation of: (a) permeate flow rate and (b) TDS using PSO-ANN.

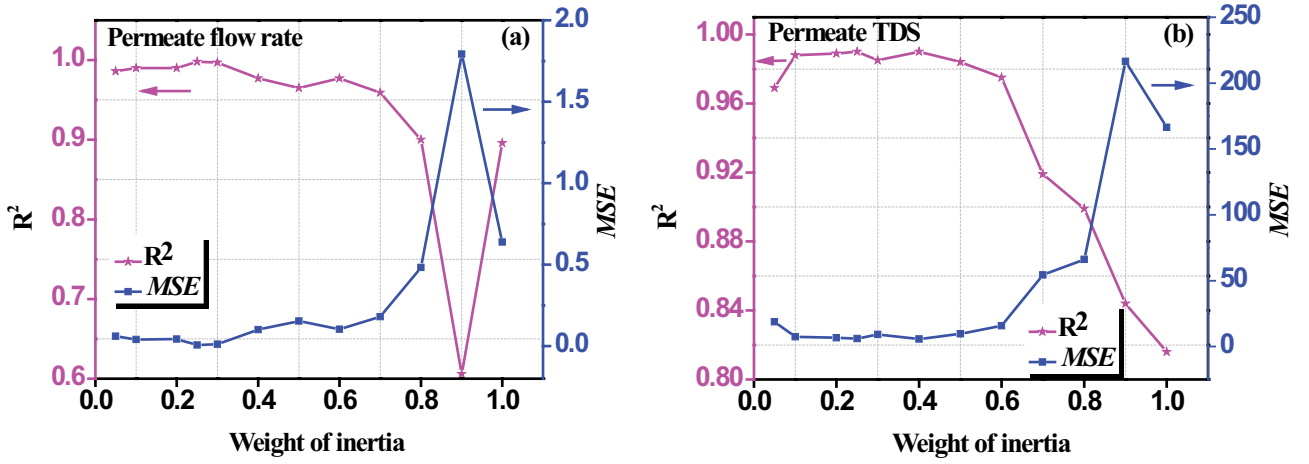

Fig. 7. Illustration of the dependence of simulation errors (MSE) and regression quality (R^2) on the weight of inertia (ω) for the case of estimation of: (a) permeate flow rate and (b) TDS using PSO-ANN.

TDS. The simulation results indicate that the performance of PSO-ANN models shows little variation before the optimum points and more deviation after that for both outputs of the desalination plant.

Armaghani et al. [37] developed a PSO-ANN model to predict tunnel boring machine performance. The authors defined the effects of c_1 and c_2 used in the PSO-ANN models. Table 2 describes the permeate flow rate and TDS performance results with variation in c_1 and c_2 using PSO-ANN models.

A choice of c_1 = 1.5 and c_2 = 2.5 gave the best performance for both the outputs permeate flow rate and permeate TDS, while a choice of c_1 = 2.5 and c_2 = 2.5 gave the poorest model fitting.

Table 2
Comparison of the performance results in terms of the permeate flow rate and TDS for different acceleration factors (c_1 and c_2) using PSO-ANN models [swarm size = 40, ω = 0.25/0.1 + rand × 0.4, n = 10]

Acceleration factors		Permeate flow rate		Permeate TDS	
c_1	c_2	R^2	MSE	R^2	MSE
0.8	3.2	0.990	0.041	0.996	2.283
1	1	0.949	0.222	0.935	39.055
1.25	1.25	0.953	0.205	0.922	46.173
1.333	2.667	0.995	0.018	0.989	6.727
1.5	1.5	0.934	0.295	0.973	16.175
1.5	**2.5**	**0.998**	**0.007**	**0.997**	**1.783**
1.714	2.286	0.989	0.048	0.994	3.643
1.75	1.75	0.973	0.119	0.966	20.632
2	2	0.996	0.015	0.994	3.540
2.286	1.714	0.995	0.020	0.983	10.002
2.667	1.333	0.987	0.058	0.991	5.323
3.2	0.8	0.939	0.271	0.983	10.269
2.5	**2.5**	**0.787**	**2.159**	**0.836**	**191.683**

Fig. 8a and b show the variation in performance parameters (R^2 and MSE) as a function of the number of nodes chosen for the hidden layer. The simulation results showed a relatively different trend than observed for ANN modeling. A choice of n = 10 demonstrated the best model performance for predicting both the permeate flow rate and TDS. The PSO-ANN parameters that yield optimum modeling of SWRO desalination plants for both outputs are summarized in Table 3.

4.1.3. FIS model simulation

FIS model performance was validated by a comparison between simulation and experimental estimates. Initially, some input data were fed to the FIS model to verify the datasets. For example, we fed the input temperature of 15°C and 50 kgf/cm² pressure to get a 4.1 L/min to permeate flow rate output. In this, a minimum variation was observed between the predicted (4.1) and the experimental results (4.0). Next, we fed the input temperature of 25°C and 60 kgf/cm² pressure to get a 68.8 ppm to permeate TDS output. Here, we have also detected the lowest variation between the predicted (68.8) and the experimental results (70.9). Finally, the surface view of all simulation results of FIS models for the permeate flow rate and TDS, as shown in Figs. 9d and 10d indicates that both outputs' obtained errors are acceptable and performing well. However, a little variation with the temperature 20°C and pressured 60 kgf/cm² for the permeate flow rate was noticed and permeate TDS have shown more dissimilarity between experimental and predicted datasets.

4.1.4. ANFIS model simulation

Similar to FIS models, the ANFIS models have been simulated, and results compared with experimental (Figs. 9e and 10e). For example, an input temperature of 15°C, and 50 kgf/cm² pressure resulted in a 4.0 L/min permeate flow rate, which is in proximity to the experimental value. Likewise, an input temperature of 25°C, and

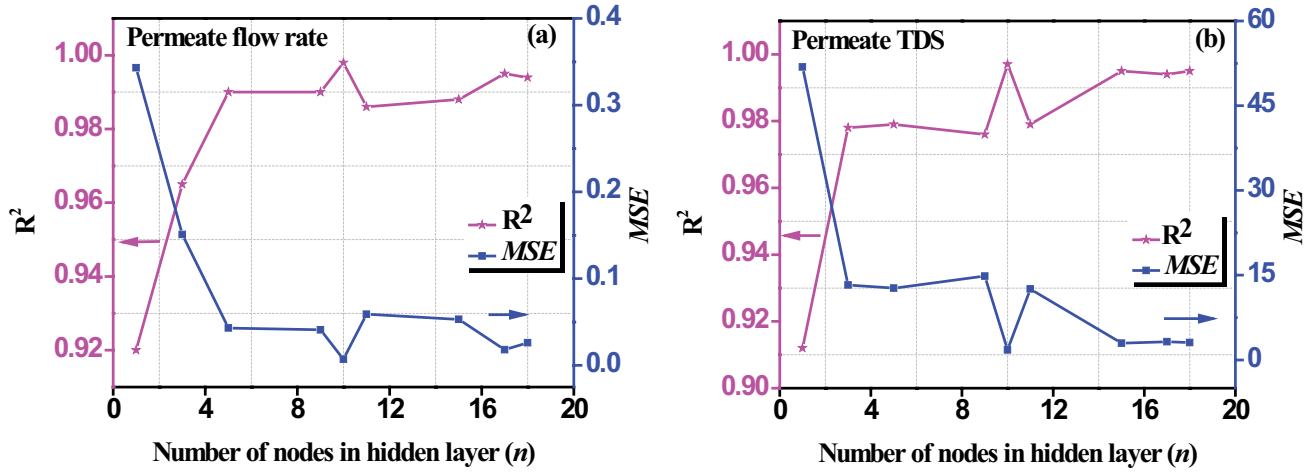

Fig. 8. Illustration of the dependence of simulation errors (MSE) and regression quality (R^2) on the number of nodes (n) in the hidden layer for the case of estimation of: (a) permeate flow rate and (b) TDS using PSO-ANN.

Table 3
Summary of the optimum model parameters for the PSO-ANN model

Factors	Model parameters	
	Permeate flow rate	Permeate TDS
Swarm size	40	40
Weight of inertia (ω)	0.25	0.1 + rand × 0.4
Acceleration factors (c_1 and c_2)	1.5, 2.5	1.5, 2.5
Number of hidden layer nodes (n)	10	10

60 kgf/cm² pressure resulted in 70.8 ppm TDS output, which is very close to the experimental value (70.9). It has been observed from simulations that the feed temperature between 10°C and 15°C shows marginally more deviations between the experimental and simulation estimates of the permeate flow rate while a minimal error was noticed for the rest of the inputs. Conclusively, the performance of ANFIS models was found to be acceptable across the entire range of operating temperatures and pressure.

4.2. Model performance

In this paper, we have proposed, optimized, and simulated four empirical models (ANN, PSO-ANN, FIS, and ANFIS) to predict the SWRO desalination plant's membrane performance. Apparently, every model has displayed good agreement between the outputs of experimental and predicted datasets. Figs. 9a and 10a show the overall performance (3D surface view) of the permeate flow rate 2.8–8.8 L/min and TDS 45.0–121.6 ppm using experimental datasets. Feed temperature range from 5°C to 30°C, and feed pressure ranges from 45 to 65 kgf/cm² have been considered to analyze the membrane's performance. The ability of the membrane's performance has been evaluated by a different combination of the varying temperatures and pressure. In this work, experimental result trends show that the permeate flow rate has been increased, and TDS has been decreased with an increased feed temperature and pressure. Figs. 9b and 10b illustrate the overall performance of the permeate flow rate (R^2 = 0.969, MSE = 0.135) and TDS (R^2 = 0.964, MSE = 21.547) using the ANN model, respectively. Here, the R^2 of the permeate flow rate has been observed marginally higher with significantly smaller errors (MSE) than the permeate TDS. The optimum number of the hidden layer nodes has been found to be 10 for this model. Further, Figs. 9c and 10c show the performance of the PSO-ANN model for permeate flow rate (R^2 = 0.998, MSE = 0.007) and TDS (R^2 = 0.997, MSE = 1.783). PSO helps generate optimum weights for ANN for the permeate flow rate and TDS of the membrane and evidently demonstrates the best results than all the other models. Moreover, Figs. 9d and 10d illustrate the performance of the permeate flow rate (R^2 = 0.952, MSE = 0.212) and TDS (R^2 = 0.949, MSE = 30.573), respectively, using the FIS model. These optimum results depend upon the designed 25 rules and the membership functions each for permeate flow rate and TDS of the plant. Finally, Figs. 9e and 10e show the performance of the permeate flow rate (R^2 = 0.926, MSE = 0.337) and TDS (R^2 = 0.948, MSE = 39.337) using the ANFIS model. ANFIS model shows the most fitting errors than the other models employed in this work.

The results of the developed models have been summarised and compared in Table 4 on the basis of two performance metrics (R^2 and MSE) with performance results of modeling attempted earlier in literature. It is apparent that the PSO-ANN model predicts experimented results more efficiently than the other models proposed in this work and literature with the highest R^2 and minimum MSE.

The results show that the PSO-ANN model performed the best among all simulated models. Thus, using this model we have developed two mathematical nonlinear model equations (Eqs. (7) and (8)) to predict the SWRO desalination plant performance using ANOVA analysis [39]. The optimal PSO-ANN model offers a more precise and accurate prediction of the membrane's performance of the plant and diagnosis variations.

Permeate flow rate, F_{pi}:

$$\begin{aligned} F_{pi} &= a_1 \times T_{fi} + a_2 \times P_{fi} + a_3 \times F_{fi} + a_4 \times C_{fi} - a_5 \times T_{fi}^2 - a_6 \times T_{fi} \times P_{fi} \\ &- a_7 \times T_{fi} \times F_{fi} + a_8 \times T_{fi} \times C_{fi} - a_9 \times P_{fi}^2 - a_{10} \times P_{fi} \times F_{fi} \\ &- a_{11} \times P_{fi} \times C_{fi} - a_{12} \times F_{fi}^2 - a_{13} \times F_{fi} \times C_{fi} - a_{14} \times C_{fi}^2 - C_1 \end{aligned} \quad (7)$$

Permeate TDS, C_{pi}:

$$\begin{aligned} F_{pi} &= b_1 \times T_{fi} + b_2 \times P_{fi} + b_3 \times F_{fi} + b_4 \times C_{fi} - b_5 \times T_{fi}^2 - b_6 \times T_{fi} \times P_{fi} \\ &- b_7 \times T_{fi} \times F_{fi} + b_8 \times T_{fi} \times C_{fi} + b_9 \times P_{fi}^2 - b_{10} \times P_{fi} \times F_{fi} \\ &- b_{11} \times P_{fi} \times C_{fi} - b_{12} \times F_{fi}^2 - b_{13} \times F_{fi} \times C_{fi} - b_{14} \times C_{fi}^2 - C_2 \end{aligned} \quad (8)$$

where T_{fi}, P_{fi}, F_{fi}, and C_{fi} are the feed temperature (°C), feed pressure (kgf/cm²), feed flow rate (L/min), and feed TDS (ppm), respectively. a_1 to a_{14} and b_1 to b_{14} are the coefficients, C_1 and C_2 are the constants for model equations of the permeate flow rate and TDS. The estimates of these constants are presented in Table 5. ANOVA analysis uses some important statistical parameters (multiple R, R^2, adjusted-R^2, and standard errors) to evaluate the goodness of fit and to verify the model equations, which are summarised in Table 6. While the fitting is evidently good, the multiple R, R^2, and adjusted-R^2 determined a relatively good fit for C_{pi} as compared to that for F_{pi}.

4.3. Model residuals/errors

It is important for the researchers to design a perfect model that offers minimum possible residuals or errors in

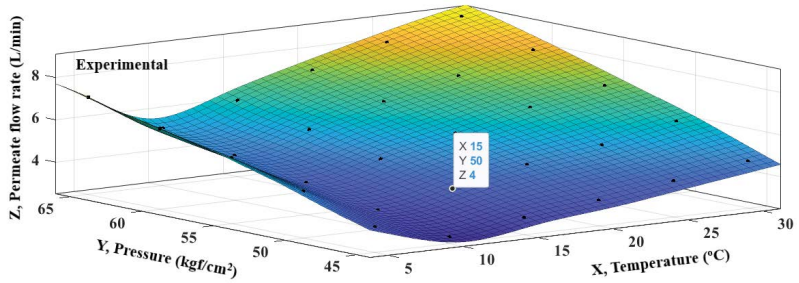

(a)

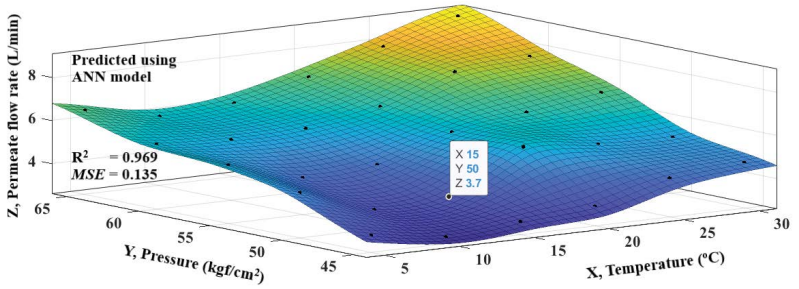

(b)

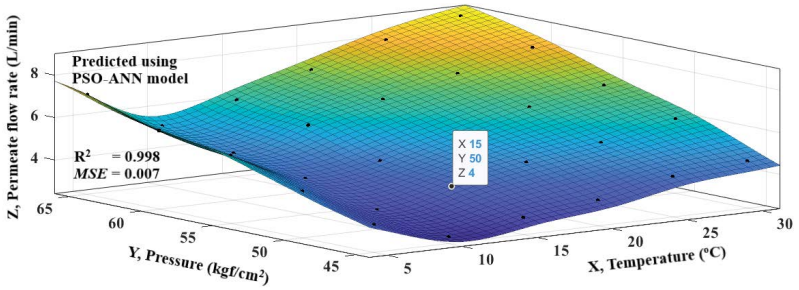

(c)

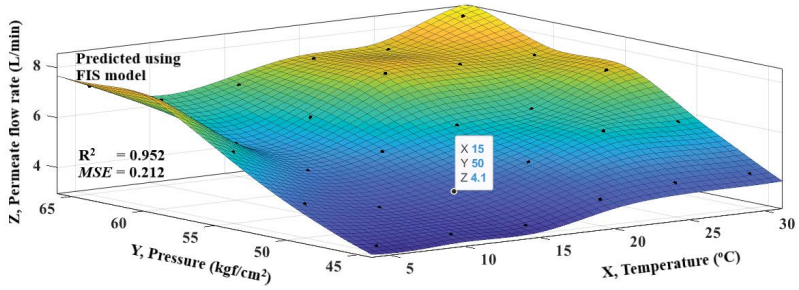

(d)

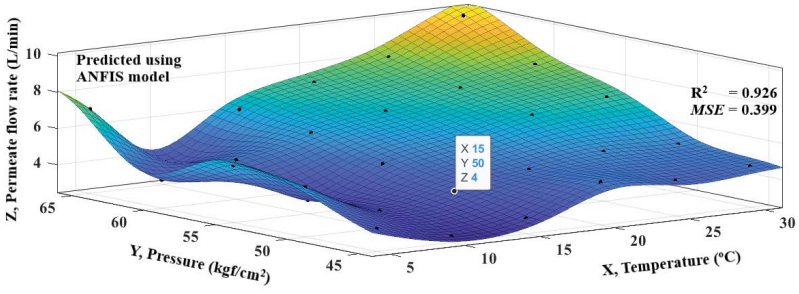

(e)

Fig. 9. Surface view comparison of permeate flow rate (L/min) for a SWRO desalination plant using (a) experimental, (b) ANN, (c) PSO-ANN, (d) FIS, and (e) ANFIS model.

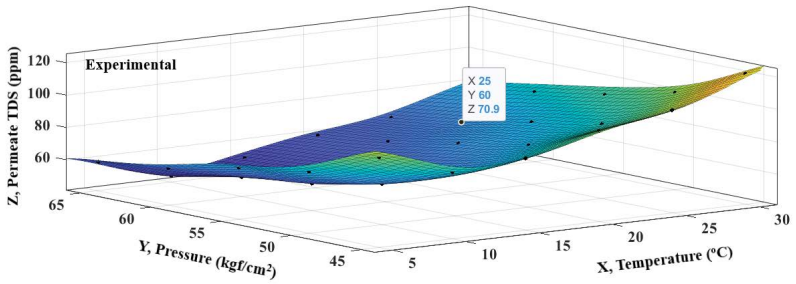

(a)

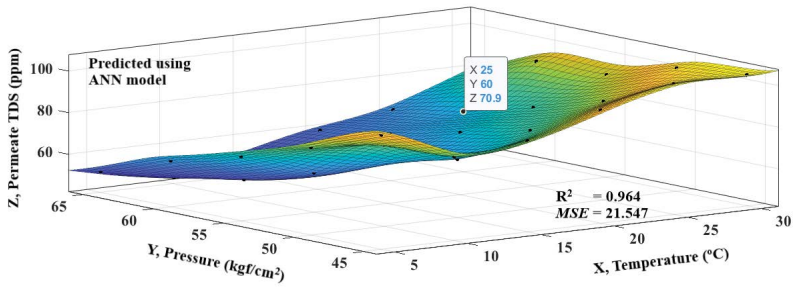

(b)

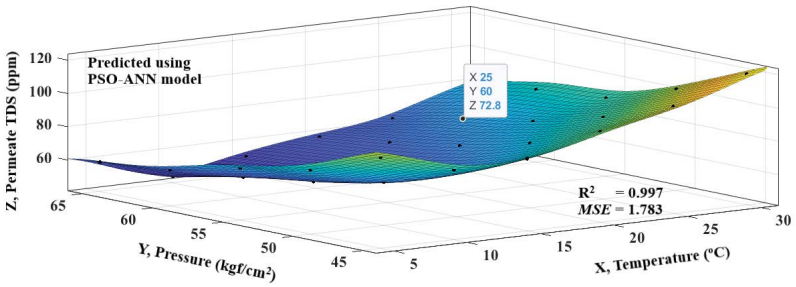

(c)

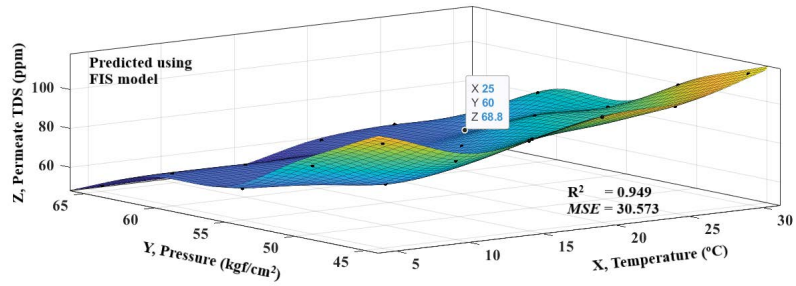

(d)

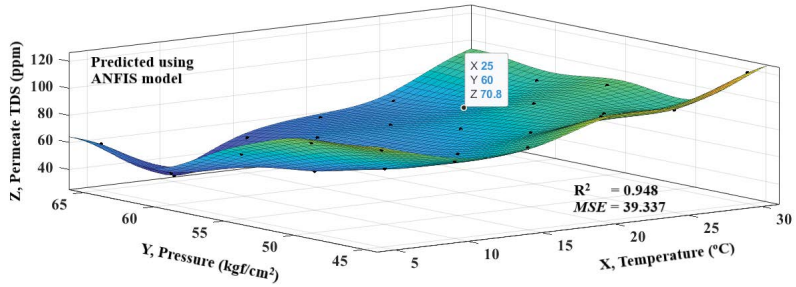

(e)

Fig. 10. Surface view comparison of permeate TDS (ppm) for a SWRO desalination plant using (a) experimental, (b) ANN, (c) PSO-ANN, (d) FIS, and (e) ANFIS model.

Table 4
Comparative analysis of performances of the developed models' (ANN, PSO-ANN, FIS, and ANFIS) and their performances with those from literature

Models		Permeate flow rate		Permeate TDS		Rank
		R^2	MSE	R^2	MSE	
Proposed work	ANN	0.969	0.135	0.964	21.547	2
	PSO-ANN	**0.998**	**0.007**	**0.997**	**1.783**	**1**
	FIS	0.952	0.212	0.949	30.573	3
	ANFIS	0.926	0.399	0.948	39.337	4
Literature						
Lee et al. [9]	ANN	0.750	0.006	0.960	–	
		NaCl rejection		Na_2SO_4 rejection		
Mahadeva et al. [38]	LM-BP-ANN	0.801	6.430	0.787	1.976	
	SCG-BP-ANN	0.807	6.417	0.821	1.660	From Memb-I
	PSO-ANN	0.821	5.854	0.828	1.588	

Remark: Salt ($NaCl/Na_2SO_4$) separation from water. Developed two poly(piperizinamide) thin-film composite membranes (Memb-I and Memb-II) in the Membrane Science and Separation Technology Division Laboratory, CSMCRI, Bhavnagar, Gujarat, India [38]

Table 5
Coefficients of the model equations of F_{pi} and C_{pi}

Parameters	F_{pi} (L/min)	C_{pi} (ppm)
	Coefficients	Coefficients
Constants	C_1 = –54,795.60015	C_2 = –600,258.5469
T_{fi}	a_1 = 17.59314643	b_1 = 362.2315155
P_{fi}	a_2 = 31.23359191	b_2 = 385.55521
F_{fi}	a_3 = 2,748.930425	b_3 = 36,160.5254
C_{fi}	a_4 = 0.792210965	b_4 = 2.851534641
T_{fi}^2	a_5 = –0.021044839	b_5 = –0.072919484
$T_{fi} \times P_{fi}$	a_6 = –0.007857212	b_6 = –0.172762675
$T_{fi} \times F_{fi}$	a_7 = –1.553452114	b_7 = –15.45661611
$T_{fi} \times C_{fi}$	a_8 = 0.000946387	b_8 = 0.003552279
P_{fi}^2	a_9 = –0.00232823	b_9 = 0.022331176
$P_{fi} \times F_{fi}$	a_{10} = –0.771423466	b_{10} = –12.22888387
$P_{fi} \times C_{fi}$	a_{11} = –0.00023716	b_{11} = –0.000651901
F_{fi}^2	a_{12} = –43.30933099	b_{12} = –565.9530309
$F_{fi} \times C_{fi}$	a_{13} = –0.002709674	b_{13} = –0.042385476
C_{fi}^2	a_{14} = –1.11988E-05	b_{14} = –2.5069E-05

Table 6
Goodness of the model equations adjustment for F_{pi} and C_{pi}

Estimator (statistical)	Condition for a good fit	F_{pi}	C_{pi}
Multiple R	Close to 1	0.983	0.995
R^2	Close to 1	0.968	0.991
Adjusted-R^2	In agreement with R^2	0.937	0.982
Standard error	Observed	0.381	2.385

predicting experimental results. This study presents four empirical models, such as ANN, PSO-ANN, FIS, and ANFIS, that have shown good agreements between experimental datasets and simulated values. However, the PSO-ANN model demonstrated the best performance with minimal residuals/errors for both outputs: permeate flow rate and TDS. A piece of such collected information for comparison among all models is presented in Fig. 11a and b. Results show that PSO-ANN is relatively more capable of generating accurate weights and bias as parameters for use in modeling to predict the best results. In general, simulation results indicate that all the remaining performed reasonably well with minimal residual errors in capturing the experimental permeate flow rate and TDS.

5. Conclusion

In this work, four empirical models based on neural network and fuzzy such as ANN, PSO-ANN, FIS, and ANFIS have been developed to predict the SWRO desalination plant's membrane performance. Developed models can be used in any type of desalination plant or related industry with a few parameter adjustments. All models consisted of four input parameters, such as feed temperature 5°C–30°C, feed pressure 45–65 kgf/cm^2, feed flow rate ~30 L/min and feed TDS ~32,000 ppm, and two output parameters as permeate flow rate 2.8–8.8 L/min and TDS 45–121.6 ppm. The trained models produced a good agreement between the experimentally reported and the predicted datasets. This work demonstrates that such models can predict accurate output with the minimal available experimental data and can be efficiently and professionally applied to investigate the membrane's performance at other operating environments and suggest suitable water production operations. Amongst all simulated models, the PSO-ANN model provides the best performance for the permeate flow rate and TDS (R^2 = 0.998, 0.997) with a minimum (MSE = 0.007, 1.783), respectively, than other models. PSO-ANN model has also demonstrated minimum residuals of almost close to zero for every set of experimental data. The modeling results show that the developed PSO-ANN model with estimated parameters may

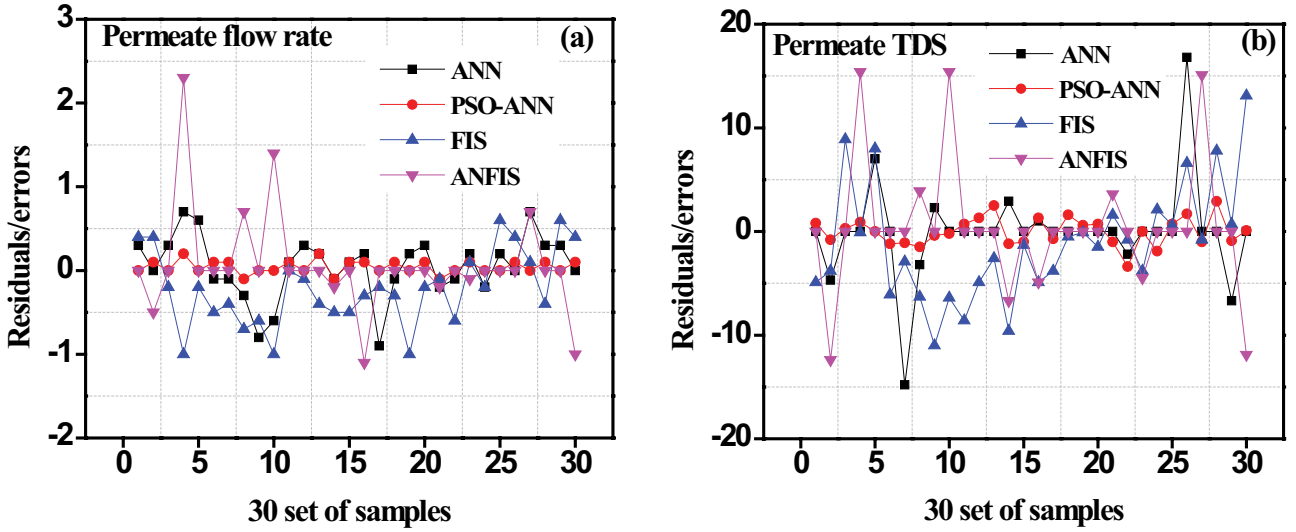

Fig. 11. Variation of model residuals: (a) predicted permeate flow rate and (b) predicted permeate TDS of the membrane using ANN, PSO-ANN, FIS, and ANFIS models.

serve as a perfect diagnostic tool for designing SWRO desalination plants to reduce time, energy, and cost.

Acknowledgments

SPP would like to acknowledge the financial support from Khalifa University through FSU-2018-29, and the Department of Education and Knowledge under "The ADEK Award for Research Excellence (AARE) 2018: AARE18-136".

References

[1] M.A. Shannon, P.W. Bohn, M. Elimelech, J.G. Georgiadis, B.J. Marĩas, A.M. Mayes, Science and technology for water purification in the coming decades, Nature, 452 (2008) 301–310.
[2] J.R. Werber, C. Osuji, M. Elimelech, Materials for next-generation desalination and water purification membranes, Nat. Rev. Mater., 1 (2016) 1–15.
[3] K. Park, J. Kim, D. Ryook, S. Hong, Towards a low-energy seawater reverse osmosis desalination plant: a review and theoretical analysis for future directions, J. Membr. Sci., 595 (2020) 1–15, doi: 10.1016/j.memsci.2019.117607.
[4] J. Kim, K. Park, D. Ryook, S. Hong, A comprehensive review of energy consumption of seawater reverse osmosis desalination plants, Appl. Energy, 254 (2019) 1–16, doi: 10.1016/j.apenergy.2019.113652.
[5] M. Al-Abri, B. Al-Ghafri, T. Bora, S. Dobretsov, J. Dutta, S. Castelletto, L. Rosa, A. Boretti, Chlorination disadvantages and alternative routes for biofouling control in reverse osmosis desalination, npj Clean Water, 2 (2019) 1–16.
[6] World Bank Group, The Role of Desalination in an Increasingly Water-Scarce World, Water Global Practice, Technical Paper, Washington DC, 2019, pp. 1–97. Available online at: https://openknowledge.worldbank.org/handle/10986/31416
[7] T. Jamieson, S.C. Leterme, Technology Influences and impacts of biofouling in SWRO desalination plants, Crit. Rev. Environ. Sci. Technol., (2020) 1–21.
[8] R. Habte, Y. Chul, M. Mezemir, B. Chul, K. Park, J. Choi, Reverse osmosis membrane fabrication and modification technologies and future trends: a review, Adv. Colloid Interface Sci., 276 (2020) 1–22, doi: 10.1016/j.cis.2019.102100.
[9] Y.G. Lee, Y.S. Lee, J.J. Jeon, S. Lee, D.R. Yang, I.S. Kim, J.H. Kim, Artificial neural network model for optimizing operation of a seawater reverse osmosis desalination plant, Desalination, 247 (2009) 180–189.
[10] Y.G. Lee, D.Y. Kim, Y.C. Kim, Y.S. Lee, D.H. Jung, M. Park, S.J. Park, S. Lee, D.R. Yang, J.H. Kim, A rapid performance diagnosis of seawater reverse osmosis membranes: simulation approach, Desal. Water Treat., 15 (2010) 11–19.
[11] M. Soltanieh, W.N. Gill, Review of reverse osmosis membranes and transport models, Chem. Eng. Commun., 12 (1981) 279–363.
[12] M. Moonkhum, Y.G. Lee, Y.S. Lee, J.H. Kim, Review of seawater natural organic matter fouling and reverse osmosis transport modeling for seawater reverse osmosis desalination, Desal. Water Treat., 15 (2010) 92–107.
[13] N.P. Padhy, S.P. Simon, Soft Computing with MATLAB Programming, Oxford University Press, USA, 2015.
[14] K.W. Chau, Particle swarm optimization training algorithm for ANNs in stage prediction of Shing Mun River, J. Hydrol., 329 (2006) 363–367.
[15] M. Buyukyildiz, G. Tezel, V. Yilmaz, Estimation of the change in lake water level by artificial intelligence methods, Water Resour. Manage., 28 (2014) 4747–4763.
[16] M. Alizamir, S. Sobhanardakani, An artificial neural network-particle swarm optimization (ANN-PSO) approach to predict heavy metals contamination in groundwater resources, Jundishapur J. Health Sci., 10 (2018) 1–8, doi: 10.5812/jjhs.67544.
[17] B. Sulugodu, P.C. Deka, Evaluating the performance of CHIRPS satellite rainfall data for streamflow forecasting, Water Resour. Manage., 33 (2019) 3913–3927.
[18] R. Mahadeva, G. Manik, O.P. Verma, S. Sinha, Modelling and simulation of desalination process using artificial neural network: a review, Desal. Water Treat., 122 (2018) 351–364.
[19] R. Mahadeva, G. Manik, A. Goel, N. Dhakal, A review of the artificial neural network based modelling and simulation approaches applied to optimize reverse osmosis desalination techniques, Desal. Water Treat., 156 (2019) 245–256.
[20] P. Gao, L. Zhang, K. Cheng, H. Zhang, A new approach to performance analysis of a seawater desalination system by an artificial neural network, Desalination, 205 (2007) 147–155.
[21] S. Al Aani, T. Bonny, S.W. Hasan, N. Hilal, Can machine language and artificial intelligence revolutionize process automation for water treatment and desalination?, Desalination, 458 (2019) 84–96.
[22] P. Cabrera, J.A. Carta, J. González, G. Melián, Wind-driven SWRO desalination prototype with and without batteries:

a performance simulation using machine learning models, Desalination, 435 (2018) 77–96.
[23] N. Voutchkov, Desalination Engineering Planning and Design, The McGraw-Hill Companies, Inc., New York, USA, 2013.
[24] M.H. Beale, M.T. Hagan, H.B. Demuth, Neural Network Toolbox, User's Guide, MathWorks, Inc., Natick MA, 2018.
[25] J. Kennedy, E. Russell, Particle swarm optimization, Proceedings of ICNN'95 – International Conference on Neural Networks, Perth WA, 1995, pp. 1942–1948.
[26] R. Eberhart, J. Kennedy, A new optimizer using particle swarm theory, Proceedings of the Sixth International Symposium on Micro Machine and Human Science, Nagoya, 1995, pp. 39–43.
[27] M. Clerc, J. Kennedy, The particle swarm-explosion, stability, and convergence in a multidimensional complex space, IEEE Trans. Evol. Comput., 6 (2002) 58–73.
[28] R.C. Eberthart, Y. Shi, Comparing Inertia Weights and Constriction Factors in Particle Swarm Optimization, Proceedings of the 2000 Congress on Evolutionary Computation. CEC00 (Cat. No.00TH8512), La Jolla CA, 2000, pp. 84–88.
[29] M.A. Ahmadi, R. Soleimani, A. Bahadori, A computational intelligence scheme for prediction equilibrium water dew point of natural gas in TEG dehydration systems, Fuel, 137 (2014) 145–154.
[30] G. Zahedi, S. Saba, M. Al-Otaibi, K.M. Yusof, Troubleshooting of crude oil desalination plant using fuzzy expert system, Desalination, 266 (2011) 162–170.
[31] I.B. Ali, M. Turki, J. Belhadj, X. Roboam, Optimized fuzzy rule-based energy management for a battery-less PV/wind-BWRO desalination system, Energy, 159 (2018) 216–228.
[32] R. Rustum, A. Mary, J. Kurichiyanil, S. Forrest, C. Sommariva, A.J. Adeloye, M.Z. Kermani, M. Scholz, Sustainability ranking of desalination plants using mamdani fuzzy logic inference systems, Sustainability, 12 (2020) 1–22.
[33] J.R. Jang, C.T.S. Sun, Neuro-fuzzy modeling and control, Proc. IEEE, 83 (1995) 378–406.
[34] H. Moayedi, A. Moatamediyan, H. Nguyen, X.N. Bui, D.T. Bui, A.S.A. Rashid, Prediction of ultimate bearing capacity through various novel evolutionary and neural network models, Eng. Comput., 36 (2020) 671–687.
[35] M. Khajeh, M. Kaykhaii, A. Sharafi, Application of PSO-artificial neural network and response surface methodology for removal of methylene blue using silver nanoparticles from water samples, J. Ind. Eng. Chem., 19 (2013) 1624–1630.
[36] M. Khajeh, A.S. Yazdi, A.F. Moghadam, Modeling of solid-phase tea waste extraction for the removal of manganese and cobalt from water samples by using PSO-artificial neural network and response surface methodology, Arabian J. Chem., 10 (2017) S1663–S1673.
[37] D.J. Armaghani, E.T. Mohamad, M.S. Narayanasamy, N. Narita, S. Yagiz, Development of hybrid intelligent models for predicting TBM penetration rate in hard rock condition, Tunnelling Underground Space Technol., 63 (2017) 29–43.
[38] R. Mahadeva, R. Mehta, G. Manik, A. Bhattacharya, An experimental and computational investigation of poly(piperizinamide) thin film composite membrane for salts separation from water using artificial neural network, Desal. Water Treat., 224 (2021) 106–121.
[39] J.D. Gil, A.R. Aguirre, L. Roca, G. Zaragoza, M. Berenguel, Prediction models to analyse the performance of a commercial-scale membrane distillation unit for desalting brines from RO plants, Desalination, 445 (2018) 15–28.